

Silica Enrichment in a Volcanic Setting Using Petrographic Analyses and Mass Balance Calculations Using Trace Element Zircon

Adil M. Wadia

Department of Geosciences, *The University of Akron Wayne College, Orrville, OH 44667, USA*

Abstract: Formulating the original composition of weathered tephra can be a challenging task. A previous study by Wadia (1998 and 2007) demonstrated the enrichment of silica according to the hypothesis that the percentage of aluminum oxide remains constant within the unweathered parent material and its weathered counterpart (Faure, 1991), which indicated the average enrichment of silica to be 6.5%. This study demonstrates the enrichment of microcrystalline-cryptocrystalline quartz in the Reid's Mistake Formation of the Newcastle Coal measures of Sydney Basin, Australia, incorporating petrographic analyses and MBC (mass balance calculations) using trace element zircon as the immobile element. For MBC, zircon is more favorable, as it is a trace element that tends to be immobile during the process of chemical weathering. The composition of the unweathered reference samples was collected from the Tertiary volcanic complexes of Northeastern New South Wales and Southeastern Queensland. ICP-AES (inductively coupled plasma-atomic emission spectroscopy) was used to determine the chemical composition of the weathered samples. The quantitative enrichment of silica was provided by performing MBC using zircon as the immobile trace element. The petrographic analyses results indicated that the tephra was subjected to chemical weathering in a meteoric regime, as represented by minerals observed in the weathered tephra. The silica enrichment by MBC involving zircon resulted in 40.11%, which is indicative of chemical weathering, and was additionally supported by the presence of chert lenses in the volcanic horizon, indicating the enrichment of silica as a result of chemical weathering.

Key words: Silica enrichment, petrographic analyses, mass balance calculations, zircon.

1. Introduction

Chert is a microcrystalline or cryptocrystalline sedimentary rock consisting mostly of interlocking crystals of quartz and is precipitated from an aqueous solution [1]. The quartz crystals are typically less than about 30 μm in diameter [2]. Although cherts are comprised of pure silica, crystalline impurities totaling less than 5% consisting of calcite, hematite, clay minerals, and organic matter are found. Cherts may form in many geochemical environments through different mechanisms; the most common ones include bedded marine chert, chert in carbonates, chert in hypersaline environments, pedogenic chert, and chert in volcanic sequences.

Chert-like rocks in volcanic sequences have also formed as a result of devitrification of silica-rich glass. Devitrification is a process where glass, which is metastable is converted to crystalline material. Baker [3] has reported the devitrification of rhyolitic glass into a chert-like rock within a volcanic sequence. Many continental volcanic sequences also contain chert lenses [4]. Such sequences are typically weathered, and chert lenses are intercalated with clay layers [4]. Their association suggests that these cherts could not have formed by hydrothermal alteration or devitrification, but by chemical weathering. A recent study by Tosca et al. [5] indicate two stages of clay formation, crystal growth and nucleation, which will contribute to the basis which will permits, Li, Mg, and Si isotope fractionalization in the process of clay precipitation. Also chemical weathering of silicates provides

Corresponding author: Adil M. Wadia, Ph.D., associate professor, research fields: geosciences and coordinator. E-mail: amwadia@uakron.edu.

important feedback regarding Earth's climate [6]. Nevertheless, large scale uncertainties with reference to distinction of silicate weathering flux from total flux, as well as sensitivity to tectonic, lithological, and climate controls remain and the geomorphological environment in which chemical weathering takes place [7, 8].

The mobility of the elements during the process of chemical weathering among certain rock forming minerals, in the order of increasing the rate of leaching from the environment is as following: (1) Ca^{2+} , Mg^{2+} , Na^+ (easily lost with leaching conditions), (2) K^+ (easily lost under leaching conditions but the rate may be slowed down as a result of fixation in the clay mineral illite structure), (3) Fe^{2+} (rate of loss is reliant on the redox potential as well as degree of leaching), (4) Si^{4+} (is slowly lost with regards to leaching conditions) (5) Ti^{4+} (may indicate limited mobility if it released from the original parent material in the form of $\text{Ti}(\text{OH})_4$, immobile in the form of TiO_2), (6) Fe^{3+} (under oxidizing conditions it is immobile), (7) Al^{3+} immobile under the pH ranging between 4.5-9.5 [9].

Formation of chert in continental volcanic sequences is poorly understood. Most cherts in this environment appear to be a product of chemical weathering. This research address the hypothesis that chert in continental volcanic sequences could be a product of chemical weathering using petrographic analyses and MBC (mass balance calculations) using trace element zircon.

To better understand the formation of chert in volcanic sequences, a case study of the chert lenses from the Reid's Mistake Formation at Swansea Head of the Newcastle Coal Measures, Sydney Basin, Australia is undertaken. The Reid's Mistake Formation has been chosen as it was characterized by the presence of tuff beds and chert lenses intercalated with paper-thin clay layers [4]. The formation is chemically weathered, which is indicated by the presence of clay layers. The silicified samples from the Reid's Mistake Formation will be examined for evidence of chemical weathering.

This will be carried out by studying the petrology and chemistry of the samples. The petrology of the samples will be studied by performing traditional thin-section microscopy.

The chemical analyses of the samples will be conducted to study the chemical compositions of the samples. These will be carried out through the ICP-AES (inductively coupled plasma-atomic emission spectroscopic analyses). The chemical data will be used to demonstrate if there has been silica enrichment in the weathered pyroclastic samples in comparison to their parent material by performing MBC using trace element zircon.

2. Study Area

The Sydney Basin occupies the southernmost region of the 2,000 km long Sydney-Gunnedah-Bowen foredeep [10, 11]. The Mount Coricudgy Anticline separates the Gunnedah Basin in the north from the Sydney Basin in the south. Within New South Wales, the Sydney Basin occupies the area between the New England Fold Belt to the northeast and the Lachlan Fold Belt to the west (Fig. 1) [12].

Structurally, the New England Fold Belt consists of a series of accretionary terranes formed along the eastern margin of a westward subducting convergent plate formed during the Late Cambrian to Permian [11, 13]. Rocks in the New England Fold (Fig. 2) consist of moderately metamorphosed volcanoclastics, basic to acidic volcanic rocks, limestone, siltstone, and marine bedded chert. The Lachlan Fold Belt consists of arenite, argillite, granite, limestone, and chert that range in age from the Cambrian to the Carboniferous [10].

Newcastle Coal Measures are of Late Permian age [14]. Besides other carbonaceous material and coal, the sediments in the Newcastle Coal Measures are composed of the following rock types: conglomerate, sandstone, shale, tuff, shaley sandstone, and sandy shale. The conglomerates contain numerous types of pebbles, viz. chert, quartzite, quartz, igneous and metamorphic rocks, coal and sandstone fragments. The

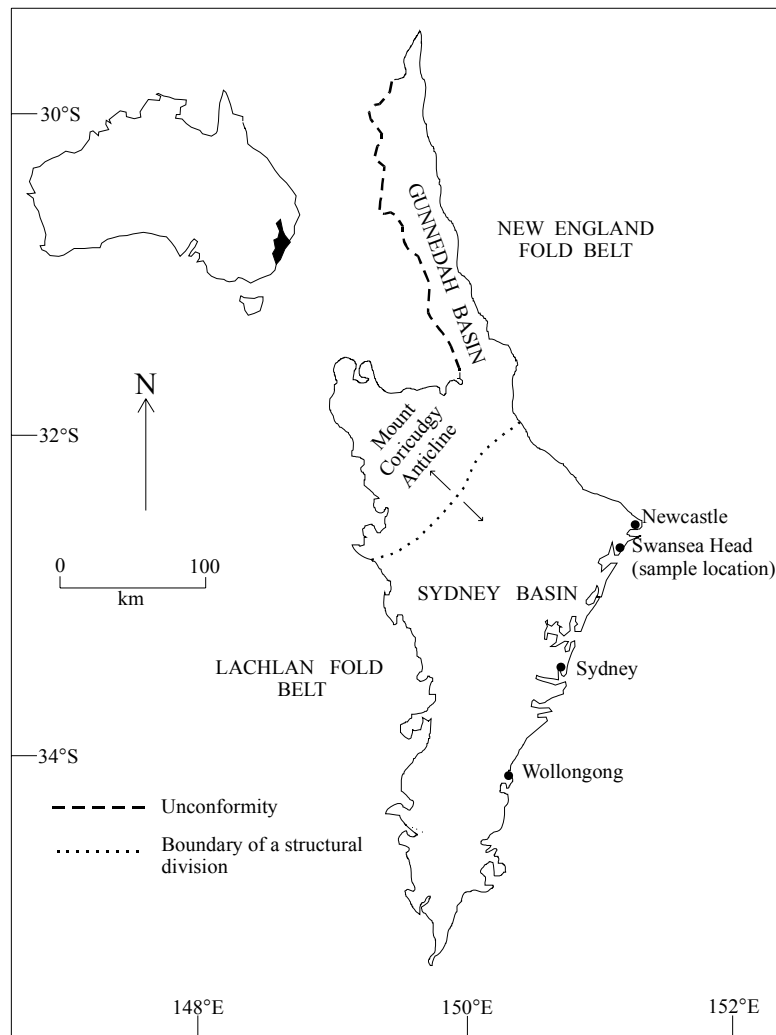


Fig. 1 A generalized map of the Sydney-Gunnedah Basin showing important geographic locations, including the study area, Swansea Head. The dotted line, a major structural element separates the Sydney Basin from the Gunnedah Basin (after Bembrick et al., 1973).

sandstones are almost entirely lithic in character. The matrix is argillaceous, however cementation by silica and carbonate is found to occur. The Newcastle Coal Measures are characterized by innumerable thin to thick bedded tuffaceous rocks. These tuffaceous rocks are found to consist of quartz, biotite, plagioclase, orthoclase, volcanic rock fragments, and glass in varying proportions. The tuff layers are typically normal graded from coarse crystal tuff at the bottom through vitric tuff to fine ashstone within a thickness of only a few centimeters [15]. A rhyolitic to rhyodacitic source is suggested for the tuffs of the Newcastle Coal Measures [15]. This coal bearing unit is divided into

the Lambton, Cardiff, Boolaroo, and Moon Island Beach Subgroups [14].

The Boolaroo Subgroup of the Newcastle Coal Measures is characterized by irregular seams of tuffs and coal seams [14]. The samples used in this study are from the Reid's Mistake Formation at Swansea Head, which is a part of the Boolaroo Subgroup and occurs in between the Lower and the Upper Pilot Coal seams [4]. The Lower Pilot Coal seam is approximately two meters in thickness and consists primarily of carbonaceous shale and silty mudstones with thin seams of vitrinite and splint coal. The Upper Pilot Coal seam is marked by fine grained chert at the base, which

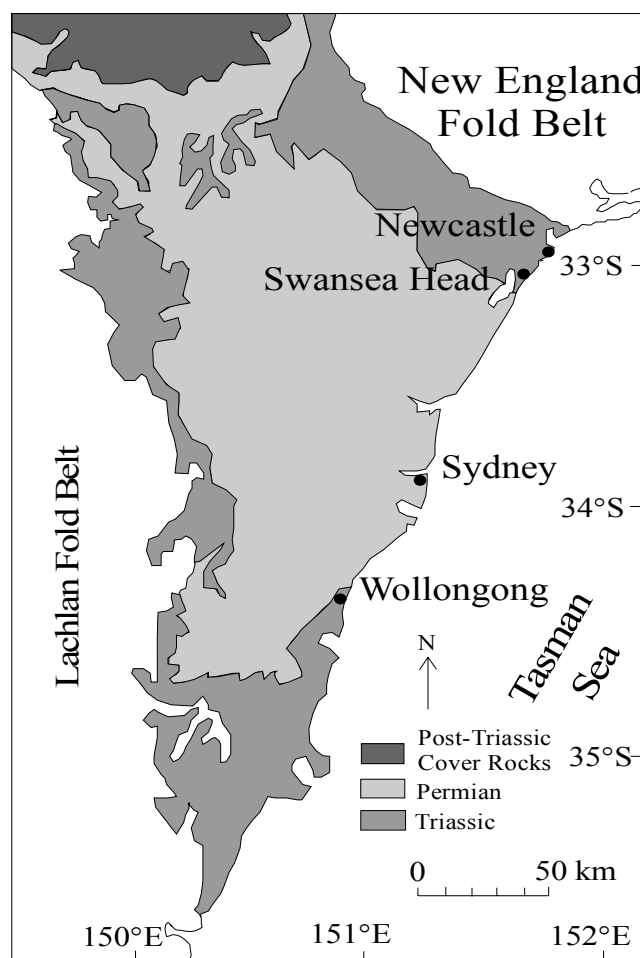


Fig. 2 A generalized geological map of the Sydney Basin (after Herbert, 1980).

is about a meter in thickness and consists of interbedded coal and claystone bands [4]. The seams are distinctive from other parts of the sequence of the Boolaroo Subgroup by the presence of a 7 meter thick tuff bed known as the Reid's Mistake Formation [14].

The Reid's Mistake Formation at Swansea Head comprises mostly a sequence of highly silicified weathered volcanic tuffs with sporadic occurrence of chert lenses and nodules [4]. Only at a few places in this sequence, paper-thin clay layers less than a millimeter in thickness are found to occur intercalated with thin chert bands (< 1 mm). Within the formation, this sequence is succeeded by about two meters of argillaceous and cherty sandstone. Overlying the argillaceous cherty sandstone is about 35 centimeters of carbonaceous shale, coal stringers, and 55

centimeters of distinct fine grained chert, which also comprises the floor of the Upper Pilot Coal Seam [4].

3. Methods

Thin-section petrography, bulk rock chemical analyses, and MBC using trace element zircon were conducted.

3.1 Petrographic Analyses

The thin-sections were prepared at the Thin-Section Laboratory, Department of Geography, Geology, and Anthropology, Indiana State University. The samples were cut perpendicular to the bedding plane using oil lubricated rock saws. Some samples were impregnated with epoxy, since they were friable. After cutting, the samples were mounted on a 1 millimeter thick glass

slide and polished to a thickness of 0.03 millimeter. The thin-sections were studied under an Olympus BHSP 2 photo-petrographic microscope. The photomicrographic system consisted of an Olympus PM-10AD exposure control unit, which was used to take the photomicrographs. A black and white film, with a film speed of 100, was used to take the photomicrographs. The photomicrographs were processed at the Photographic Laboratory, Indiana State University. Seven thin-sections from seven samples were studied under a petrographic microscope to obtain detailed information regarding the mineralogical composition and textural relationships between minerals. In the textural study, the focus was on the dissolution/replacement of phenocryst minerals, glass shards, and precipitation of fine-grained microcrystalline-cryptocrystalline quartz.

3.2 Rock Chemistry

The whole rock chemical analyses were performed in order to obtain the weight percentages of major oxides and to determine the loss and gain of elements in weathered samples with respect to the original composition of the parent.

Since the entire pyroclastic deposit was weathered, the original composition of the parent rock could not be obtained. Owing to this limitation, a hypothetical reference rock was selected for comparison with the weathered pyroclastic samples. The composition of the tephra of Reid's Mistake Formation was suggested to range from rhyolite to a rhyodacite [15]. Since the parent rocks of the weathered samples were not available for comparison, an average of eight unweathered samples was selected as the reference rock. The reference rock consisted of eight rhyolite samples, two of which were from Springbrook and six from Binna Burra of Tertiary central volcanic complexes in southeast Queensland and northeast New South Wales [16]. Though the samples ranged in composition from rhyolitic to rhyodacitic, the composition of the reference rock selected was

rhyolitic, in order to demonstrate the minimum enrichment in SiO_2 . The whole rock chemistry of all samples was carried out through ICP-AES. The samples for analyses were crushed using a diamonite mortar and pestle, and passed through a 100 mesh sieve. The Diamonite mortar and pestle was used in order to avoid any contamination. The samples were shipped to Acme Analytical Laboratory in Vancouver, Canada for ICP-AES. The error for the entire analysis was correct to $\pm 2\%$. The in-house standard (SO15) used by Acme Analytical Laboratory consisted of a rock that was basic in composition as compared to the specimens under consideration. According to the assayers of the Acme Analytical Laboratory, the accuracy and precision of the analyses was not affected by the standard used [17].

3.3 Mass Balance Calculations

Chemical weathering rates are traditionally inferred in two ways from the field data gathers. The first method involves the catchment mass balance, where weathering rates are calculated by subtracting the chemical fluxes in atmospheric deposition in streamflow. The second method is the mass balance approach, where weathering rates are calculated via depletion of mobile elements with respect to immobile ones [18]. The second method is used in this study.

Mass balance calculations were performed in order to find out the gain or loss of the major oxides and the LOI (loss on ignition) relative to a reference rock which serves as a hypothetical parent material to the samples analyses. The calculations were based on the method described by Faure [19]. The losses and gains of oxides and LOI rested on the assumption that the amount of one major oxide had remained constant throughout, although its concentration could have changed a little [19]. Following Faure [19], instead of Al_2O_3 , Zr was selected to be the element that remained constant, which is a standard procedure in low-temperature geochemical calculations. The amounts of various oxides and Zr remaining in the

samples under consideration were calculated by multiplying their percent concentrations obtained from chemical analyses by the weight loss factor (w). The concentrations of all oxides in the reference rock as well as the samples under consideration were normalized to 100%, prior to the calculation of the weight loss factor. The weight loss factor was obtained from the ratio of the concentration of the constant element (Zr) in the reference rock (fresh sample) to the concentration of Zr in the samples under consideration (weathered samples), which is given by the following equation: $w = (Zr)_{\text{reference rock}} \div (Zr)_{\text{weathered rock samples}}$.

The average value of each oxide component in the weathered samples was determined. Subsequently, the loss and gains of each oxide and Zr was compared with that of the reference rock.

4. Results

4.1 Thin-Section Petrography

Quartz is the most dominant mineral in all samples. Volcanic quartz occurring as phenocryst is observed in a matrix consisting mostly of microcrystalline (grain size 5-30 microns) to cryptocrystalline quartz (grain size less than five microns). Volcanic quartz was identified by its straight extinction, occasional euhedral form and embayments (Figs. 3 (a); (b)). Fine grained quartz was identified by its low relief, low birefringence and first order gray interference color [20]. Most samples show porphyritic texture.

Besides volcanic quartz, plagioclase feldspars, and biotite have also been observed as phenocrysts in samples (Figs. 3 (a); (b)). Plagioclase feldspar was recognized on the basis of low relief and polysynthetic twinning (Fig. 4). Biotite was identified by its one set of perfect cleavage and showing pleochroic colors from light to dark brown [21]. Alteration of biotite is observed in most thin-sections. Biotite alteration is always associated with iron oxide. The latter, stains the biotite grains as well as the area around biotite (Figs. 3 (a); (b)). At times, iron oxide occurs as thin veins (hematitic veins) that cut across the groundmass

consisting of microcrystalline to cryptocrystalline quartz (Fig. 5).

Among clay minerals, kaolinite and illite have been identified under the polarizing microscope. Kaolinite occurs as equant grains and shows first order interference

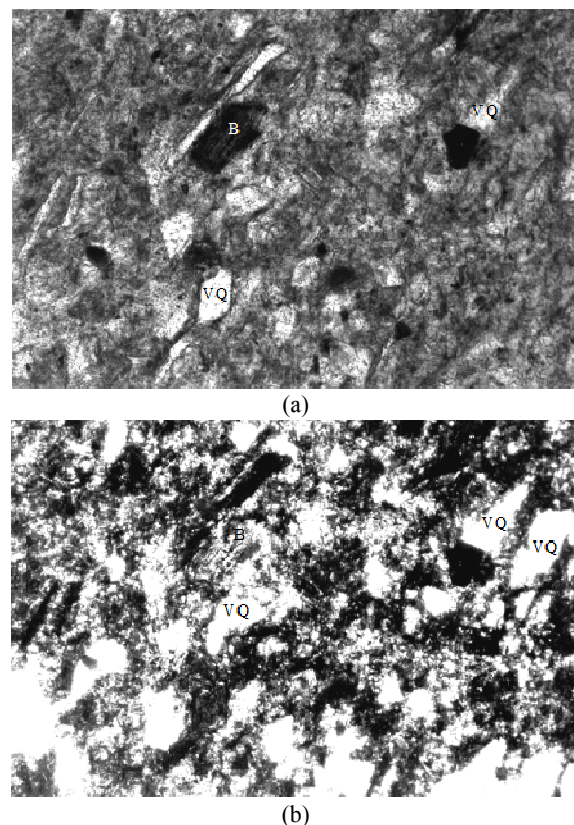


Fig. 3 The (a) section is photomicrograph of the sample under plane polarized light. The (b) section is the photomicrograph under crossed polars. The photographs indicate phenocrysts of VQ (volcanic quartz) and B (biotite).



Fig. 4 This section is photomicrograph under crossed polars. The figure shows intense replacement of PF (plagioclase feldspar) by microcrystalline-cryptocrystalline quartz.

color of gray. The equant kaolinite looks similar to microcrystalline quartz but is differentiated by the presence of fine hair like lines representing kaolinite booklets. However, kaolinite is mostly altered to illite during burial diagenesis [22, 23]. Illite shows an elongated crystal habit, well developed cleavage and higher birefringence colors of first order yellow (Fig. 6). Many glass shards, originally glassy, are observed to be filled up by microcrystalline-cryptocrystalline quartz (Fig. 7 (a); (b)). Dissolution of phenocrysts like plagioclase feldspars and volcanic quartz is common in all samples [24] and dissolution rates have indicated to decrease over time [25].

4.2 Rock Chemistry and Chemical Composition

The chemical analyses of all seven samples were conducted to determine the weight percentage of major

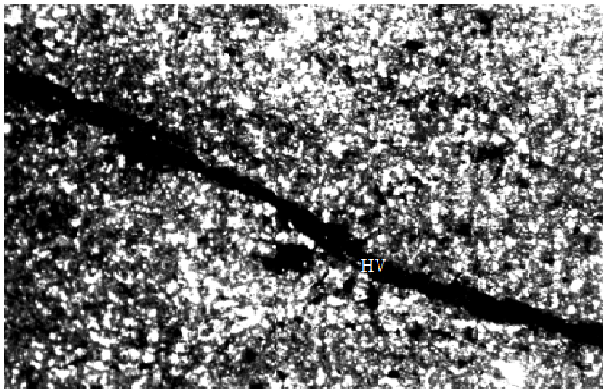


Fig. 5 This section is photomicrograph under crossed polars. The sample indicates the presence of hematitic vein.

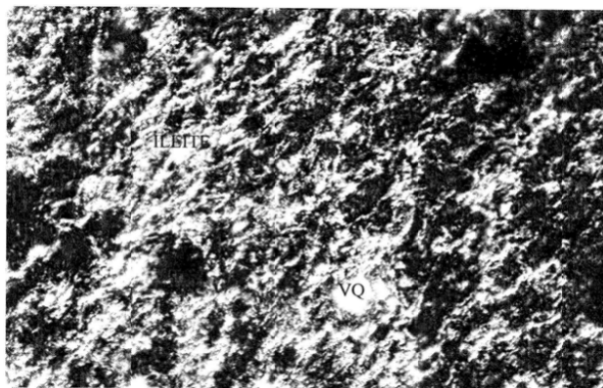
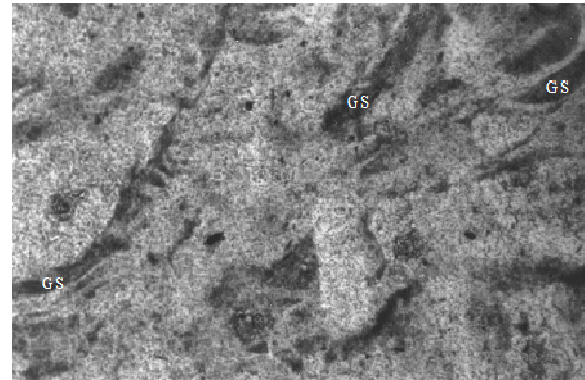
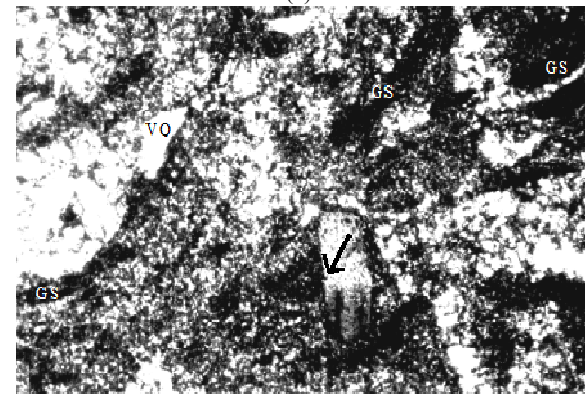


Fig. 6 This section is photomicrograph under crossed polars. The sample shows porphyritic texture where volcanic quartz as a phenocryst in a matrix comprising illite and microcrystalline-cryptocrystalline quartz.



(a)



(b)

Fig. 7 The (a) section is photomicrograph under plane polarized light. The (b) section is photomicrograph of sample under crossed polars. The figures indicate the presence of glass shards in a groundmass consisting of microcrystalline to cryptocrystalline quartz.

oxides and LOI. Based on the chemical analyses, mass balance calculations between the reference rock and the pyroclastic samples were conducted. Due to the absence of the parent rock, the average composition of the pyroclastic samples is compared with the average composition of the hypothetical parent, the reference rock. Mass balance calculations are carried out between the average composition of the pyroclastic samples and the reference rock.

A few studies have been conducted on the Reid's Mistake Formation; however, none addressed the chemistry of the formation. The data from chemical analyses are provided in Table 1. The range of the composition of the reference rock, including the average and the standard deviation, is given in Table 2. The standard deviation for the pyroclastic samples, as well as the reference rock, is calculated using the

unbiased (n-1) method. It is important to establish a comparison between the average composition from which the reference rock was obtained and the average of the samples gathered from chemical analyses of the samples. Marginally higher SiO₂, Fe₂O₃, MgO, and LOI content relative to the reference rock have been observed. On the other hand, CaO, Na₂O, and K₂O show lower values compared to the reference rock (Tables 2 and 3).

4.3 Mass Balance Calculations

Mass balance between the pyroclastic samples and the reference rock was calculated in order to establish

the effects of chemical weathering. Chemical weathering, in a weathering profile will result in depletion of mobile elements and the enrichment of immobile ones. These calculations were performed by taking an average of all the oxides and Zr for the specimens instead of calculating them individually. The basis for doing so was that according to the assumption, the amount of Zr must remain constant. However, the weight percentage of Zr in the weathered specimens ranged from 83.00 to 179.00 parts per million (ppm). The average weight percentage of Zr for the weathered specimens is 129.44 ppm, which is close to that of the reference rock (157.63 ppm). The average

Table 1 The chemical composition of weathered pyroclastic samples.

| Oxides | SB27 | SB28 | SB29 | SB31 | SB34 | SB35 | SB36 | AVG | STD | SO15 | Ref. |
|--------------------------------|-------|-------|-------|-------|--------|--------|--------|----------|------|-------|-------|
| SiO ₂ | 73.23 | 67.95 | 78.83 | 74.43 | 81.56 | 82.21 | 76.98 | 76.46 | 5.03 | 48.88 | 74.63 |
| TiO ₂ | 0.14 | 0.16 | 0.07 | 0.08 | 0.08 | 0.10 | 0.40 | 0.15 | 0.12 | 1.74 | 0.11 |
| Al ₂ O ₃ | 13.29 | 15.85 | 10.06 | 10.45 | 9.03 | 9.84 | 11.58 | 11.44 | 2.39 | 12.63 | 11.90 |
| Fe ₂ O ₃ | 1.60 | 1.47 | 0.53 | 2.65 | 0.29 | 0.31 | 0.27 | 1.02 | 0.92 | 7.23 | 0.75 |
| MnO | 0.02 | 0.01 | 0.01 | 0.03 | < 0.01 | < 0.01 | < 0.01 | 0.01 | 0.01 | 1.30 | 0.02 |
| MgO | 0.85 | 1.00 | 0.07 | 0.25 | 0.07 | 0.14 | 0.21 | 0.37 | 0.39 | 7.37 | 0.06 |
| CaO | 0.19 | 0.22 | 0.27 | 0.15 | 0.20 | 0.26 | 0.05 | 0.19 | 0.07 | 5.60 | 0.46 |
| Na ₂ O | 0.73 | 0.66 | 4.94 | 4.58 | 4.14 | 3.74 | 0.64 | 2.78 | 2.00 | 2.46 | 3.26 |
| K ₂ O | 2.43 | 3.07 | 1.05 | 0.63 | 1.30 | 1.99 | 7.46 | 2.56 | 2.32 | 1.85 | 5.09 |
| P ₂ O ₅ | 0.04 | 0.05 | 0.03 | 0.04 | 0.05 | 0.01 | 0.04 | 0.04 | 0.01 | 2.90 | 0.02 |
| LOI | 7.90 | 8.90 | 4.50 | 6.10 | 3.60 | 1.70 | 2.50 | 5.03 | 2.71 | 5.90 | 2.99 |
| | | | | | | | Total | ~ 100.00 | | | |

AVG and STD are the average and standard deviation of samples. The sample SO15 is the Acme Analytical Laboratories in-house standard.

Table 2 The average composition of the reference rock.

| Oxides | Q75 | S74 | PU11 | 13 | Q71 | LP32 | LP18 | PU35 | AVG | STD |
|--------------------------------|-------|-------|-------|-------|-------|-------|-------|----------|-------|------|
| SiO ₂ | 73.83 | 73.85 | 74.52 | 73.86 | 74.10 | 75.64 | 74.46 | 76.77 | 74.63 | 1.05 |
| TiO ₂ | 0.15 | 0.36 | 0.07 | 0.07 | 0.06 | 0.06 | 0.07 | 0.07 | 0.11 | 0.10 |
| Al ₂ O ₃ | 11.00 | 11.98 | 11.66 | 11.54 | 12.11 | 12.45 | 12.45 | 12.00 | 11.90 | 0.49 |
| Fe ₂ O ₃ | 0.68 | 0.89 | 0.69 | 0.64 | 0.64 | 0.41 | 1.19 | 0.89 | 0.75 | 0.23 |
| MnO | 0.01 | 0.03 | 0.02 | 0.02 | 0.01 | 0.01 | 0.01 | 0.01 | 0.02 | 0.01 |
| MgO | 0.07 | 0.23 | 0.03 | 0.01 | 0.03 | 0.03 | 0.05 | 0.05 | 0.06 | 0.07 |
| CaO | 0.56 | 0.40 | 0.57 | 0.54 | 0.60 | 0.31 | 0.29 | 0.41 | 0.46 | 0.12 |
| Na ₂ O | 2.69 | 3.57 | 3.55 | 3.63 | 2.80 | 3.28 | 2.82 | 3.70 | 3.26 | 0.42 |
| K ₂ O | 5.00 | 4.99 | 5.18 | 5.10 | 5.49 | 5.04 | 5.10 | 4.84 | 5.09 | 0.19 |
| P ₂ O ₅ | 0.03 | 0.06 | 0.01 | 0.01 | 0.00 | 0.02 | 0.01 | 0.02 | 0.02 | 0.02 |
| LOI | 5.66 | 2.18 | 3.39 | 3.54 | 3.68 | 1.75 | 2.76 | 0.92 | 2.99 | 1.44 |
| | | | | | | | Total | ~ 100.00 | | |

AVG is the average and STD is the standard deviation of the major oxide composition of the reference rock. Q75 and S74 are Springbrook rhyolites and PU11, 13, Q71, LP32, LP18 and PU35 are Binna Burra rhyolites from Tertiary volcanic complexes in southeast Queensland and northeast New South Wales (from Ewart and others, 1976). LOI is given as the sum of H₂O (+) and H₂O (-).

Table 3 Mass balance calculations using Zr as the immobile trace element.

| Oxides & Zr | AVG-Ref (Oxides % mass), (Zr ppm) | AVG-Ref (Norm) | AVG-Sam (Oxides % mass), (Zr ppm) | AVG-Sam (Norm) | AMT-Rem | G/L (gm) | G/L (%) |
|--------------------------------|-----------------------------------|----------------|-----------------------------------|----------------|---------|----------|---------|
| SiO ₂ | 74.63 | 29.05 | 76.46 | 33.36 | 40.70 | 11.65 | 40.11 |
| TiO ₂ | 0.11 | 0.04 | 0.15 | 0.07 | 0.08 | 0.04 | 86.49 |
| Al ₂ O ₃ | 11.90 | 4.63 | 11.44 | 4.99 | 6.09 | 1.46 | 31.47 |
| Fe ₂ O ₃ | 0.75 | 0.29 | 1.02 | 0.45 | 0.54 | 0.25 | 85.99 |
| MnO | 0.02 | 0.01 | 0.01 | 0.00 | 0.01 | 0.00 | -31.62 |
| MgO | 0.06 | 0.02 | 0.37 | 0.16 | 0.20 | 0.17 | 743.36 |
| CaO | 0.46 | 0.18 | 0.19 | 0.08 | 0.10 | -0.08 | -43.51 |
| Na ₂ O | 3.26 | 1.27 | 2.78 | 1.21 | 1.48 | 0.21 | 16.62 |
| K ₂ O | 5.09 | 1.98 | 2.56 | 1.12 | 1.36 | -0.62 | -31.22 |
| P ₂ O ₅ | 0.02 | 0.01 | 0.04 | 0.02 | 0.02 | 0.01 | 173.52 |
| LOI | 2.99 | 1.16 | 5.03 | 2.19 | 2.68 | 1.51 | 130.07 |
| Zr | 157.63 | 61.35 | 129.14 | 56.35 | 68.74 | 7.39 | 12.04 |
| Total | 256.92 | 100.00 | 229.19 | 100.00 | | | |

composition of the pyroclastic samples was also selected owing to the absence of the parent material as discussed earlier. The amount of oxide remaining was calculated by multiplying the percentage of each oxide by the weight loss factor (w) using the equation. A summary of these calculations is provided in Table 3 [26].

$$w = (\text{Zr})_{\text{reference rock}} \div (\text{Zr})_{\text{weathered rock samples}}$$

$$w = 157.63/129.14 = 1.22$$

5. Discussion and Conclusion

In order to establish the chemical maturity of these rocks, it is essential that the chemical compositions of the parent rocks are known. This study attempts to reconstruct the original composition of the parent material by using Zr as immobile trace element from the weathered pyroclastic deposits. The compositions of the parent material are then used to compare with the composition of the weathered pyroclastic samples. Based on the immobile trace elemental composition Zr, the compositions of the original pyroclastic rocks are obtained.

On the basis of the data gathered, the following conclusions are made:

The widespread occurrence of secondary minerals like microcrystalline-cryptocrystalline quartz along with clay minerals suggests that chemical weathering was responsible for the formation of silicified

chert-like rocks in the Reid's Mistake Formation.

Textural evidence, such as the dissolution of primary minerals like volcanic quartz, feldspars, and glass shards also indicates chemical weathering.

Chemical weathering is also indicated by the presence of clay minerals such as kaolinite and illite, which are common products of weathering, as evidenced from thin-section petrography.

Using Zr as the immobile trace element indicates the enrichment of silica via the process of chemical weathering in a volcanic setting.

For future studies, supplementing petrography with scanning electron microscopic studies could be implemented. This would be especially helpful in confirming the presence of clay minerals and in detecting the textural relationships of the primary and secondary minerals in greater detail and clarity.

References

- [1] Blatt, H., and Tracy, R. J. 1996. *Petrology Igneous, Sedimentary and Metamorphic* (Second Edition). New York: W. H. Freeman and Company.
- [2] Jackson, J. A. 1997. *Glossary of Geology*. Alexandria, Virginia: American Geological Institute, 769.
- [3] Baker, G. 1959. "Opal Phytoliths in Some Victorian Soils and "Red Rain" Residues." *Australian Journal of Botany* 7: 64-87.
- [4] Loughnan, F. C., and Ray, A. S. 1978. "The Reid's Mistake Formation at Swansea Head, New South Wales." *Journal of the Geological Society of Australia* 25 (8):

- 473-81.
- [5] Tosca, R. L., Tosca, N. J., and Tipper, E. T. 2015. "Experimental Determination of Mg, Si and Li Isotope Fractionalization during Clay Mineral Formation." Presented at the Goldschmidt Conference, Prague, CZ.
- [6] Bickle, M., Chapman, H., Tipper, E., Galy, A., De La Rocha, C., and Ahman, T. 2015. "Chemical Weathering in the Flood Plain of Ganges." Presented at the Goldschmidt Conference, Prague, CZ.
- [7] Ameijeiras-Mariño, Y., Opfergelt, S., Delmelle, P., De Jong, J., and Vanacker, V. 2015. "Assessing the Impact of Denudation Rate on Soil Chemical Weathering Intensity: The Response of Si Isotopes." Presented at the Goldschmidt Conference, Prague, CZ.
- [8] Bouchez, J., Gaillaudet, J., Lupker, M., Louvat, P., France-Lanord, C., Maurice, L., Armijos, E., and Moquet, J.-S. 2012. "Floodplains of Large Rivers: Weathering Reactors or Simple Silos?" *Chemical Geology* 332-3 (November): 166-84.
- [9] Loughnan, F. C. 1969. *Chemical Weathering of Silicate Minerals*. New York: American Elsevier Publishing Company, 1154.
- [10] Herbert, C. 1980. "Depositional Development of the Sydney Basin." In *A Guide to the Sydney Basin*, edited by Herbert, C., and Helby, R. Vol. 26. Sydney: New South Wales Geological Survey Bulletin, 11-52.
- [11] Scheibner, E. 1985. "Suspect Terrains in the Tasman Fold Belt, Eastern Australia." In *Tectonostrati Graphic Terrains of the Circum-Pacific Regions*, edited by David, H. G. Houston: Circum-Pacific Council for Energy and Mineral Resources, 493-514.
- [12] Bembrick, C. S., Herbert, C., Scheibner, E., and Stuntz, J. 1973. "Structural Subdivision of the New South Wales Portion of the Sydney-Bowen Basin." *New South Wales Geological Survey-Quarterly Notes* 11: 1-13
- [13] Cawood, P. A. 1982. "Structural Relations in the Subduction Complex of the Paleozoic New England Fold Belt, Eastern Australia." *Journal of Geology* 90 (4): 381-92.
- [14] McKenzie, P. J., and Britten, R. A. 1969. "Newcastle Coal Measures (the Sydney Basin)." *Journal of Geological Society of Australia* 16 (1): 339-50.
- [15] Diessel, C. F. K. 1983. "Tuffs and Tonsteins in the Coal Measures of New South Wales, Australia." In *Proceedings of the CR 10 Int Congr Carbon Strat Geol*, 197-211.
- [16] Ewart, A., Oversby, V. M., and Mateen, A. 1977. "Petrology and Isotope Geochemistry of Tertiary Lavas from the Northern Flank of the Tweed Volcano, Southeastern Queensland." *Journal of Petrology* 18 (1): 73-113.
- [17] Gravel, J. L. 1997. *Acme Analytical Laboratories Ltd*. 852 E. Hastings St. Vancouver, BC Canada V6A 1R6. (Personal Communication)
- [18] Kirchner, J. W., and Riebe, C. S. 2015. "Chemical Weathering Rates Viewed from Twin Perspectives of Soils and Surface Waters." Presented at the Goldschmidt Conference, Prague, CZ.
- [19] Faure, G. 1991. *Principles and Applications of Inorganic Geochemistry*. New York: Macmillan Publishing Company.
- [20] Wadia, A. M. 1998. "Chemical Weathering of Volcanic Ash as a Probable Origin of Chert in the Reid's Mistake Formation of the Newcastle Coal Measures, Sydney Basin." Master thesis, Indiana State University.
- [21] Phillips, W. R., and Griffen, D. T. 1981. *Optical Mineralogy the Nonopaque Minerals*. San Francisco: W. H. Freeman and Company, 677.
- [22] Dutta, P. K., and Suttner, L. J. 1986. "Alluvial Sandstone Composition and Paleoclimate, II. Authigenic Mineralogy." *Journal of Sedimentary Petrology* 56 (3): 346-58.
- [23] Hower, J., Eslinger, E. V., Hower, M. E., and Perry, E. A. 1976. "Mechanism of Burial Metamorphism of Argillaceous Sediment: 1. Mineralogical and Chemical Evidence." *Geological Society of America Bulletin* 87 (5): 725-37.
- [24] Wadia, A. M. 2007. "Can Chemical Weathering of Volcanic Ash Result in the Formation of Chert?" *Geological Society of America Abstracts with Programs* 39 (6): 506.
- [25] White, A. F., and Brantley, S. L. 2003. "The Effect of Time on the Weathering of Silicate Minerals: Why Do Weathering Rates Differ in the Laboratory and Field?" *Chemical Geology* 202 (December): 479-506.
- [26] Wadia, A. M. 2013. "Mass Balance Calculations Using Trace Element Zircon to Indicate Silica Enrichment in a Volcanic Setting, (Advances in Quantitative Sediment Provenance Research: Novel Approaches from Multi-proxy Provenance Data to Provenance Modeling I)." *125th Anniversary of Geological Society of America, Geological Society of America Annual Meeting Abstracts with Programs* 45 (7).